Am J Physiol Endocrinol Metab 297: E184–E193, 2009.
First published May 5, 2009; doi:10.1152/ajpendo.00163.2009.

Haploinsufficiency of the retinoblastoma protein gene reduces diet-induced obesity, insulin resistance, and hepatosteatosis in mice

Josep Mercader,[1] Joan Ribot,[1] Incoronata Murano,[2] Søren Feddersen,[3] Saverio Cinti,[2] Lise Madsen,[4,5] Karsten Kristiansen,[3,5] M. Luisa Bonet,[1] and Andreu Palou[1]

[1]*Laboratory of Molecular Biology, Nutrition, and Biotechnology, Universitat de les Illes Balears and Centro de Investigación Biomédica en Red Fisiopatología de la Obesidad y Nutrición, Palma de Mallorca, Spain;* [2]*Department of Molecular Pathology and Innovative Therapies, Faculty of Medicine, University of Ancona (Politecnica delle Marche), Ancona, Italy;* [3]*Department of Biochemistry and Molecular Biology, University of Southern Denmark, Odense, Denmark;* [4]*National Institute of Nutrition and Seafood Research, Bergen, Norway; and* [5]*Department of Biology, University of Copenhagen, Copenhagen, Denmark*

Submitted 12 March 2009; accepted in final form 28 April 2009

Mercader J, Ribot J, Murano I, Feddersen S, Cinti S, Madsen L, Kristiansen K, Bonet ML, Palou A. Haploinsufficiency of the retinoblastoma protein gene reduces diet-induced obesity, insulin resistance, and hepatosteatosis in mice. *Am J Physiol Endocrinol Metab* 297: E184–E193, 2009. First published May 5, 2009; doi:10.1152/ajpendo.00163.2009.—Brown adipose tissue activity dissipates energy as heat, and there is evidence that lack of the retinoblastoma protein (pRb) may favor the development of the brown adipocyte phenotype in adipose cells. In this work we assessed the impact of germ line haploinsufficiency of the pRb gene (Rb) on the response to high-fat diet feeding in mice. $Rb^{+/-}$ mice had body weight and adiposity indistinguishable from that of wild-type ($Rb^{+/+}$) littermates when maintained on a standard diet, yet they gained less body weight and body fat after long-term high-fat diet feeding coupled with reduced feed efficiency and increased rectal temperature. Rb haploinsufficiency ameliorated insulin resistance and hepatosteatosis after high-fat diet in male mice, in which these disturbances were more marked than in females. Compared with wild-type littermates, $Rb^{+/-}$ mice fed a high-fat diet displayed higher expression of peroxisome proliferator-activated receptor (PPAR)γ as well as of genes involved in mitochondrial function, cAMP sensitivity, brown adipocyte determination, and tissue vascularization in white adipose tissue depots. Furthermore, $Rb^{+/-}$ mice exhibited signs of enhanced activation of brown adipose tissue and higher expression levels of PPARα in liver and of PPARδ in skeletal muscle, suggestive of an increased capability for fatty acid oxidation in these tissues. These findings support a role for pRb in modulating whole body energy metabolism and the plasticity of the adipose tissues in vivo and constitute first evidence that partial deficiency in the Rb gene protects against the development of obesity and associated metabolic disturbances.

brown adipose tissue; white adipose tissue; energy metabolism; genetic animal model

THE RETINOBLASTOMA PROTEIN (pRb), encoded by the Rb gene, plays an important role in the control of cell cycle, apoptosis, and cell differentiation (7, 23). In particular, pRb is involved in the control of adipocyte biology. Both inhibitory and stimulatory effects of pRb on white adipogenesis have been described in adipocyte cell models. On the one hand, there is evidence that active pRb may behave as a transcriptional corepressor of peroxisome proliferator-activated receptor (PPAR)γ (8), a nuclear receptor pivotal for adipogenesis (31). On the other hand, it has been shown that white adipocyte precursor cells lacking pRb exhibit a defective adipose conversion in response to standard hormonal stimulation (3, 5, 33), a defect that can be bypassed by ligand (rosiglitazone)-induced activation of PPARγ (14). Active pRb may facilitate adipogenesis by triggering permanent cell cycle exit required for terminal differentiation (35), by enhancing the transcriptional activity of the proadipogenic CCAAT/enhancer-binding proteins (C/EBPs) through a direct protein-protein interaction (5, 25, 26, 29), and through effects on mitogen-activated protein kinase pathways (13).

In addition, pRb appears to exert an inhibitory effect specifically on brown adipogenesis and has been proposed to act as a molecular switch between white and brown adipocyte differentiation (12). Unlike wild-type precursor cells, precursor cells lacking pRb differentiate in culture into adipocytes that express brown adipocyte-specific genes, such as the uncoupling protein 1 (UCP1) gene and the PPAR coactivator-1α (PGC-1α) gene, and have an increased mitochondrial content (12). Modulated absence or inactivation of pRb appears to provide a window permissible for brown adipocyte differentiation that is critically dependent on an increased sensitivity of the differentiating cells to cAMP (12). Lack or inactivation of pRb may also facilitate the remodeling of white adipocytes toward a brown-like phenotype in vivo. In fact, it has been shown that adipose tissue-specific homozygous ablation of the Rb gene in adult mice leads to the acquisition of brown adipose tissue (BAT)-like features in white adipose tissue (WAT) depots (6) and that treatments promoting increased oxidative metabolism in white adipocytes (both in vivo and in cell models), such as cold exposure or retinoic acid administration, are accompanied by a downregulation of the expression and/or inactivation of the pRb (12, 21, 22, 29).

Effects of pRb in modulating adipogenesis and the metabolic plasticity of adipose tissues may have important implications for whole body energy metabolism. In this work, we have used mice with germ line haploinsufficiency of the Rb gene ($Rb^{+/-}$ mice) that, unlike $Rb^{-/-}$ mice, are viable (2, 16) as an as-yet unexplored model to study the role of pRb in energy metabolism and adipocyte biology in vivo, and we present novel evidence that Rb haploinsufficiency confers protection against diabesity after long-term high-fat diet feeding.

Address for reprint requests and other correspondence: M. L. Bonet, Edifici Mateu Orfila, Universitat de les Illes Balears, Cra. Valldemossa Km 7.5, 07122 Palma de Mallorca, Spain (e-mail: luisabonet@uib.es).

MATERIALS AND METHODS

Animals

Wild-type ($Rb^{+/+}$) and $Rb1^{tm1Tyj}$ ($Rb^{+/-}$) C57BL/6J mice were from the Jackson Laboratory (Bar Harbor, ME). All $Rb^{+/-}$ mice and wild-type control mice used in this work were from litters obtained by mating $Rb^{+/-}$ females to wild-type males. Litters were genotyped by PCR of DNA extracted from tail biopsies using primers sets as indicated by the provider. Unless otherwise indicated, animals were housed at 22°C with a 12:12-h light-dark cycle (lights on at 0800) and free access to food and water.

Experimental Design

Feeding experiments. Three conditions were studied: *1*) 7-wk-old $Rb^{+/+}$ ($n = 8$) and $Rb^{+/-}$ ($n = 7$) male mice fed from weaning until euthanization a standard chow diet with 8% of the energy as fat (Panlab, Barcelona, Spain), *2*) 19-wk-old $Rb^{+/+}$ ($n = 7$) and $Rb^{+/-}$ ($n = 7$) male mice fed the standard chow until 7 wk of age and thereafter a high-fat diet with 45% of the energy as fat (HFD45; from Research Diets, New Brunswick, NJ), and *3*) 25-wk-old male ($n = 9$) and female ($n = 10$) $Rb^{+/+}$ and male ($n = 6$) and female ($n = 6$) $Rb^{+/-}$ mice fed the standard chow until 7 wk of age and thereafter a high-fat diet with 60% of the energy as fat (HFD60; also from Research Diets). Energy intake was estimated on a per-cage basis from the actual amount of food consumed by the animals and its caloric equivalence. Rectal temperature was measured within the first 4 h of the light cycle using a digital thermometer (RS, Barcelona, Spain). Animals were killed by decapitation under fed conditions within the first 2 h of the light cycle. Liver, skeletal muscle (gastrocnemius), interscapular BAT, and WAT depots were dissected, weighed, and frozen at −80°C until analysis. Serum was prepared from blood collected from the neck and stored at −20°C until analysis.

Cold experiment. Fourteen-week-old $Rb^{+/+}$ ($n = 9$) and $Rb^{+/-}$ ($n = 10$) female mice maintained on the standard chow diet were acclimated to thermoneutrality (30°C) for 14 days before being placed in a cold room (6°C). Rectal temperature was measured at the indicated times of exposure to the cold. All animal experimentation was conducted in accord with accepted standards of humane animal care, and the protocols were approved by the University of the Balearic Islands Bioethics Committee.

Light Microscopy, Morphometric Analysis, and UCP1 Immunohistochemistry

Tissue samples (pituitary, lung, liver, BAT, inguinal WAT, and retroperitoneal WAT) from wild-type and $Rb^{+/-}$ mice were fixed by immersion in 4% paraformaldehyde in 0.1 M sodium phosphate buffer, pH 7.4, overnight at 4°C, dehydrated, cleared, and paraffin embedded so that the plane of section corresponded with the one of the wider surfaces. Three-micrometer-thick sections at the same level were obtained and stained with hematoxylin-eosin to assess morphology. No signs of neoplasia were found in tissues of $Rb^{+/-}$ mice examined at the end of the HFD60 feeding period. The area of unilocular adipocytes was measured on hematoxylin-eosin-stained adipose tissue sections, at ×20 magnification under the light microscopy, using the Nikon Lucia Image program. Immunohistochemical demonstration of UCP1 was performed in BAT sections according to the avidin-biotin-peroxidase complex method (15) using a polyclonal anti-rat UCP1 antibody raised in sheep as primary antibody (kindly provided by Dr. D. Ricquier, Paris, France). Negative controls were performed by substituting the primary antibody with sheep IgG. No cross-reaction with UCP2 and UCP3 was observed in tissues expressing the highest levels of UCP2 (liver) and UCP3 (skeletal muscle).

Blood Parameters

Serum insulin, leptin, and total adiponectin concentrations were measured using enzyme-linked immunosorbent assay kits (from DRG Instruments, Marburg, Germany; R & D Systems, Minneapolis, MN; and Phoenix Europe, Karlsruhe, Germany, respectively). Serum nonesterified fatty acids (NEFA), triacylglycerol, and glycerol levels were measured using enzymatic colorimetric kits (Wako Chemicals, Neuss, Germany; and Sigma, Madrid, Spain). Blood glucose was measured using an Accu-Chek Glucometer (Roche Diagnostics, Barcelona, Spain).

Assessment of Glucose Tolerance and Insulin Resistance

Glucose tolerance was assessed as described previously (10). Insulin resistance was assessed by the homeostatic model assessment for insulin resistance (HOMA-IR) after the animals had been submitted to a 6-h fast (from 2400 to 0600). Although originally developed and validated in humans, evidence has been presented that HOMA-IR can be used as a surrogate index to roughly determine insulin sensitivity and resistance in mice (17). HOMA-IR score was calculated from fasting insulin and glucose concentrations as described (20).

Tissue Lipids

Total tissue lipids were extracted and quantified according to a previously published procedure (30). Triacylglycerol content was measured in the lipid extract using a commercial enzymatic kit (Sigma).

Gene Expression Analysis

Total RNA was extracted from tissues using Trizol reagent (Invitrogen, Carlsbad, CA) according to the supplier's instructions. mRNA expression levels were analyzed by real-time PCR using the LightCycler System with SYBR Green I sequence nonspecific detection (Roche Diagnostics, Mannheim, Germany) on cDNA synthesized from total tissue RNA. The sequences of the primer sets used are compiled in Supplemental Table S1 (Supplemental Material for this article can be found at the *AJP-Endocrinology and Metabolism* web site). Relative gene expression was calculated using the $2^{\Delta\Delta C_T}$ method (18), with β-actin as reference gene.

Immunoblotting Analysis

UCP1 was analyzed in BAT samples by immunoblotting as described (22), using rabbit anti-mouse UCP1 antibody (Alpha Diagnostics, San Antonio, TX) as primary antibody and horseradish peroxidase-conjugated anti-rabbit IgG antibody (Amersham Biosciences) as secondary antibody. Amido black B10 staining of blots prior to development provided visual evidence for equal loading and blotting of proteins. For pRb analysis, preparation of extracts from mouse tissue, electrophoresis, blotting, and visualization was performed essentially as described (14). As primary antibodies, mouse anti-human pRb antibody (PharMingen, San Diego, CA) and rabbit anti-mouse Brg-1 antibody (Santa Cruz Biotechnology, Santa Cruz, CA) were used at a 1:1,000 and 1:500 dilution, respectively. Secondary antibodies were horseradish peroxidase-conjugated anti-mouse or anti-rabbit IgG antibodies (DAKO, Glostrup, Denmark).

Statistical Analysis

Data are expressed as means ± SE. Statistical significance of differences between genotype groups was assessed by two-tailed Student's *t*-test, or, where indicated, two-way ANOVA was used to determine the significance of effects of genotype, sex, and possible genotype × sex interactions. Threshold of significance was set at $P < 0.05$.

RESULTS

Rb Haploinsufficiency Confers Relative Protection Against High-Fat Diet-Induced Obesity

Seven-week-old $Rb^{+/-}$ mice fed regular chow had body weight and fat content indistinguishable from wild-type control littermates, as did $Rb^{+/-}$ mice fed HFD45 for 12 wk from 7 wk of age (data not shown). However, after a prolonged dietary challenge (18 wk on HFD60 from 7 wk of age), $Rb^{+/-}$ mice attained 10% lower body weight and 22 (males) to 30% (females) lower percentage of body fat than wild-type littermates (Fig. 1*A*). Individual fat pad weights (Fig. 1*B*), mean adipocyte size (Fig. 1*C*), and leptinemia (Table 1) were lower in the $Rb^{+/-}$ mice. Body weight gain in $Rb^{+/+}$ and $Rb^{+/-}$ mice first began to diverge after several weeks on HFD60 (Fig. 2*A*). Cumulative food intake was unchanged in the $Rb^{+/-}$ males and slightly reduced (by 6% at the end of the HFD60 feeding period) in the $Rb^{+/-}$ females compared with wild-type controls (Fig. 2*B*). Feed efficiency (body weight gained/calories consumed) was consistently lower in the $Rb^{+/-}$ mice than in wild-type littermates along the feeding period with HFD60 (Fig. 2*C*). Rectal temperature measured in the last week of HFD60 feeding was significantly higher in the $Rb^{+/-}$ mice (Fig. 1*D*). Of note, rectal temperature was already increased or tended so in (female) $Rb^{+/-}$ mice fed the standard chow diet (37.6 ± 0.2 vs. 36.6 ± 0.4°C; $n = 9$–10/group, $P = 0.058$) and in (male) $Rb^{+/-}$ mice fed HFD45 for 12 wk (39.2 ± 0.2 vs. 38.7 ± 0.1°C; $n = 7$/group, $P = 0.026$), when there were no differences in body weight and adiposity between Rb genotype groups. In addition, $Rb^{+/-}$ mice maintained on standard chow better resisted the transient drop in rectal temperature that accompanies exposure to a cold environment (Fig. 1*E*).

Rb Haploinsufficiency Confers Relative Protection Against High-Fat Diet-Induced Insulin Resistance

After 14 wk on HFD60, compared with wild-type sex-matched littermates, $Rb^{+/-}$ male mice exhibited better glucose tolerance (Fig. 3*A*) and were more insulin sensitive and less insulin resistant,

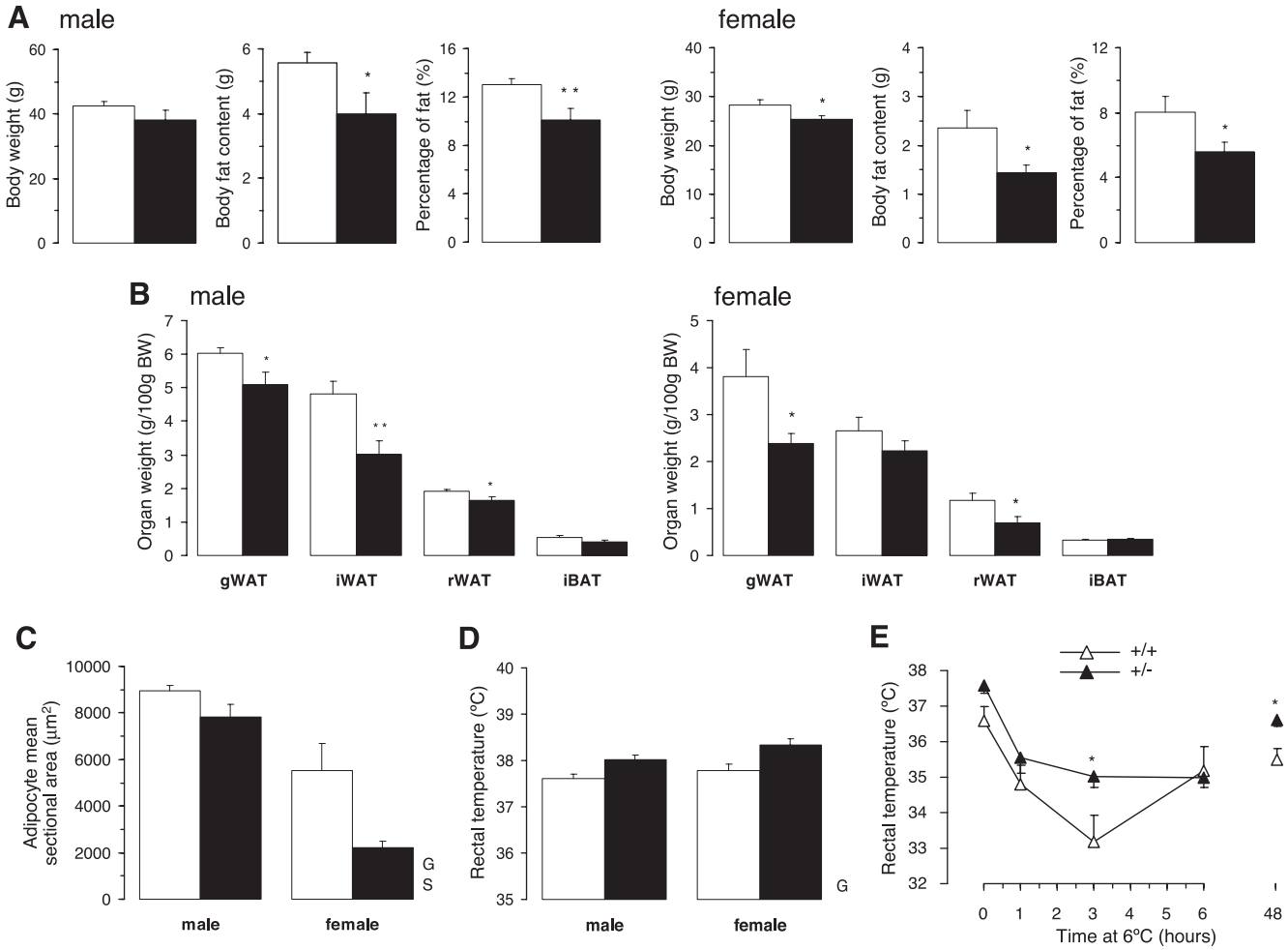

Fig. 1. Haploinsufficiency of the retinoblastoma protein gene (Rb) reduces obesity after high-fat diet feeding and increases energy expenditure. *A*: body weight, body fat content, and %fat in wild-type and $Rb^{+/-}$ mice after 18 wk on a high-fat diet with 60% of the energy provided as fat (HFD60). *B*: comparison of gonadal white adipose tissue (gWAT), inguinal WAT (iWAT), retroperitoneal WAT (rWAT), and interscapular BAT (iBAT) weights/body weights between wild-type and $Rb^{+/-}$ mice after 18 wk on HFD60. *C*: mean adipocyte sectional area in rWAT of wild-type and $Rb^{+/-}$ mice after 18 wk on HFD60. *D*: rectal temperature in wild-type and $Rb^{+/-}$ mice after 17 wk on HFD60. *E*: time course of rectal temperature in wild-type and $Rb^{+/-}$ female mice fed standard chow upon exposure to a cold environment (6°C). Data are the mean ± SE of 6–10 animals/group (*A*, *B*, and *D*), 3 animals/group (*C*), and 9–10 animals/group and time point (*E*). Open bars, wild-type mice; filled bars, $Rb^{+/-}$ mice. * and **Different from wild-type group ($P < 0.05$ and $P < 0.01$, respectively; Student's *t*-test). G and S, significant effect of genotype and sex, respectively, in 2-way ANOVA ($P < 0.05$).

Table 1. *Serum parameters in the fed state in $Rb^{+/-}$ and wild-type mice after 18 wk of being fed a high-fat diet where 60% of the energy was provided as fat*

	Males		Females		
	Wild type	$Rb^{+/-}$	Wild type	$Rb^{+/-}$	2-Way ANOVA
Glucose, mM	7.02±0.34	6.63±0.39	8.2±0.28	7.3±0.92	
Insulin, μg/l	2.92±0.76	1.74±0.52	0.60±0.07	0.64±0.18	S ($P = 0.002$)
Leptin, ng/ml	62.6±5.0	40.6±8.9	20.3±4.0	10.7±1.3	G ($P = 0.009$), S ($P = 0.000$)
Adiponectin, μg/ml	16.8±1.2	13.4±0.9	22.9±0.6	23.8±1.3	S ($P = 0.000$)
Triacylglycerol, mg/dl	140±10	169±30	86±8	96±13	S ($P = 0.000$)
NEFA, mM	1.45±0.10	1.08±0.09*	1.01±0.07	1.21±0.12	G × S ($P = 0.005$)
Glycerol, mg/ml	0.51±0.05	0.50±0.08	0.32±0.05	0.49±0.11	

Data are the mean ± SE of 6–10 animals/group. Rb, retinoblastoma protein gene; S, effect of sex; G, effect of genotype; G × S, interaction between sex and genotype; NEFA, nonesterified fatty acids. *Different from sex-matched wild-type group ($P < 0.05$; Student's *t*-test).

as indicated by a 2.4-fold lower HOMA-IR index (Fig. 3*B*). These effects were not found in the female mice, in which glucose tolerance and insulin sensitivity after HFD60 were not as impaired as in the males [note that, 3 h after glucose injection, blood glucose levels had returned to basal values in the wild-type females but remained high in the wild-type males (Fig. 3*A*) and that the HOMA-IR index was much higher in the male than in the female wild-type mice (Fig. 3*B*)].

In line with a link between Rb haploinsufficiency and improved insulin sensitivity, after 18 wk on HFD60 $Rb^{+/-}$ male mice displayed significantly reduced serum NEFA levels and a trend toward reduced fed insulinemia in the face of unchanged glycemia compared with wild-type littermates (Table 1). These changes were absent or attenuated in the $Rb^{+/-}$ female mice (Table 1). Serum triacylglycerol, glycerol, and total adiponectin levels after HFD60 were not affected by Rb haploinsufficiency in either sex (Table 1). Of note, 7-wk-old $Rb^{+/-}$ male mice fed the standard chow diet already displayed reduced fed insulinemia (0.75 ± 0.14 vs. 1.06 ± 0.17 μg/l, $P = 0.023$) in the face of unchanged glycemia (10.8 ± 1.2 vs. 10.9 ± 0.9 mM) compared with wild-type littermates, suggestive of a higher insulin sensitivity in the Rb heterozygous mice.

Rb Haploinsufficiency Confers Relative Protection Against High-Fat Diet-Induced Hepatosteatosis

Macroscopic appearance of liver (paler in the wild-type mice) and morphological examination of liver sections showed that hepatosteatosis after 18 wk on HFD60 was markedly reduced in $Rb^{+/-}$ male mice compared with wild-type controls (Fig. 4, *A* and *B*). In accordance, liver total lipid content and triacylglycerol content were reduced in the $Rb^{+/-}$ male mice by 60 and 47%, respectively (Fig. 4*C*). Hepatosteatosis after HFD60 was not apparent in the females (Fig. 4*B*), in which the effect of Rb haploinsufficiency on liver lipids was not as marked as in the males (Fig. 4*C*). Absolute liver weight, but not liver weight as percentage of body weight, was lower in $Rb^{+/-}$ mice of both sexes than in wild-type littermates (Fig. 4*D*). Skeletal muscle triacylglycerol content after HFD60 was unaffected by the Rb genotype (data not shown).

Rb-Haploinsufficient Mice Have Reduced pRb Protein Expression Levels in Adipose Tissues and Signs of Increased Metabolism After High-Fat Diet Feeding Compared With Wild-Type Mice

Gene expression changes in line with increased metabolism were found in WAT depots of the $Rb^{+/-}$ mice after 18 wk on HFD60, in keeping with their reduced development of dietary obesity compared with wild-type littermates. This is shown in Fig. 5 for the inguinal WAT depot; similar results were obtained in the retroperitoneal WAT depot (Supplementary Table S2). In particular, inguinal WAT of $Rb^{+/-}$ mice presented with four- to sixfold increased mRNA levels of PGC-1α, a transcriptional cofactor for expression of the UCP1 gene and genes related to mitochondria biogenesis and function (11, 27), and of cytochrome oxidase subunit II (COX-II), a component of the mitochondrial respiratory chain, and with more modestly yet significantly increased mRNA levels of nuclear respiratory factor 1 (NRF1), a PGC-1α-coactivated transcription factor for mitochondria-related nuclear genes, including the NRF1 gene itself (19); PRDM16, a marker of the brown adipocyte lineage that may function as an activator of PGC-1 isoforms through protein-protein interactions (34); and cAMP-dependent protein kinase A (PKA) regulatory subunit Iα (RIα), whose enrichment can trigger changes in PKA holoenzyme composition, resulting in a lower threshold for activation by cAMP (1, 4). Expression of the forkhead transcription factor FOXC2, which positively controls the RIα gene and whose enforced expression in adipose tissues of transgenic mice results in WAT-to-BAT transformation and a lean phenotype (1), was increased in the retroperitoneal WAT of the $Rb^{+/-}$ mice (Supplementary Table S2) and tended to be increased in the inguinal WAT of the female mutants (Fig. 5). A stimulatory effect of Rb haploinsufficency on UCP1 mRNA levels in WAT depots did not reach statistical significance (Fig. 5 and Supplementary Table S2). Histological examination suggested increased vascularization in WAT of the $Rb^{+/-}$ mutants (not shown) that was supported by increased expression of vascular endothelial growth factor (VEGF) mRNA both in the inguinal and the retroperitoneal depot (Fig. 5 and Supplementary Table S2). Interestingly, together with the increased expression of energy metabolism-related genes we found an increased expression of the proadipogenic/lipogenic transcription factor PPARγ in WAT depots of the $Rb^{+/-}$ mice (Fig. 5 and Supplementary Table S2). Importantly, expression levels of pRb protein in WAT depots as measured by immunoblotting were reduced in $Rb^{+/-}$ mice to approximately one-half of the levels found in wild-type littermates (shown in Fig. 6 for the inguinal depot).

As in WAT, signs of increased metabolism relative to wild-type littermates were apparent in BAT of the $Rb^{+/-}$ mice after HFD60. First, morphological examination revealed a reduced lipid content and lipid droplet size in BAT of the $Rb^{+/-}$

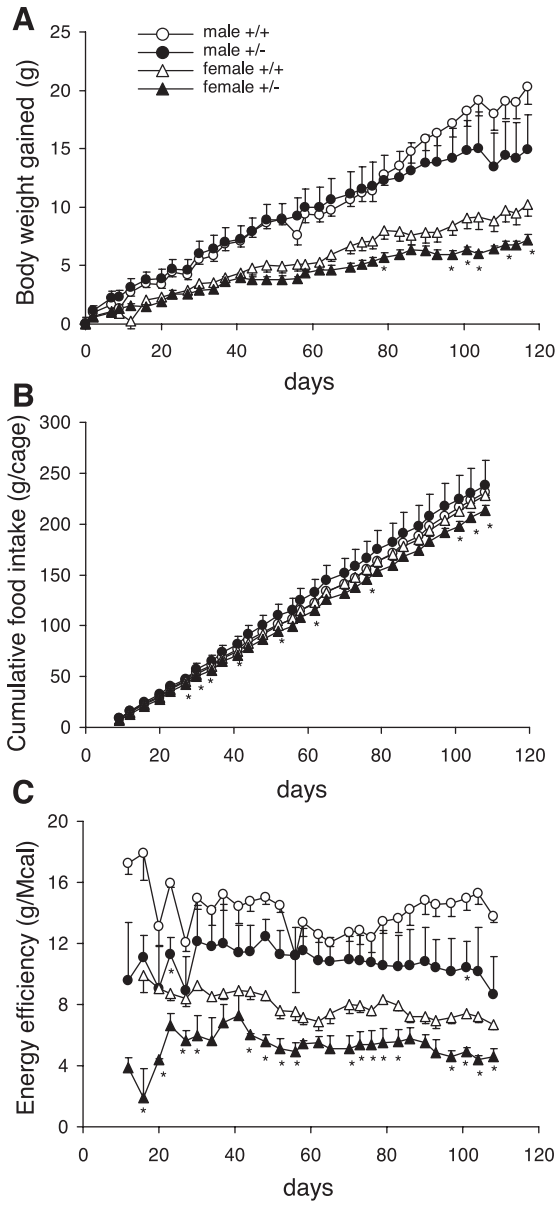

Fig. 2. Body weight gain (*A*), cumulative food intake (*B*), and energy efficiency (*C*) in wild-type and $Rb^{+/-}$ mice along with 17 wk of HFD60. Body weight gain data are the mean ± SE of 6–10 animals/group. Cumulative food intake and energy efficiency were calculated on a per-cage basis and are the mean ± SE of 2–3 cages/group (3–4 animals/cage). *Different from sex-matched wild-type group ($P < 0.05$; Student's *t*-test).

mice, which was particularly evident in the males (Fig. 7*A*). In addition, BAT of the $Rb^{+/-}$ mice contained increased levels of UCP1 protein as measured by immunoblotting, an effect that reached statistical significance in the males (Fig. 7*B*). Finally, at the mRNA level, BAT of the $Rb^{+/-}$ mice exhibited an increased expression of RIα, in line with a more easily activated thermogenesis, as well as of PRDM16, and, in the females, also NRF1 (Supplementary Table S2).

We also compared the expression of selected genes in liver and skeletal muscle of $Rb^{+/-}$ and $Rb^{+/+}$ male mice after 18 wk on HFD60 in an attempt to evaluate the eventual contribution of changes in lipid metabolism in these tissues to the reduced obesity and improved metabolic profile observed in the $Rb^{+/-}$ male mice. The mRNA levels of PPARα, which plays a critical role in the transcriptional control of fatty acid oxidation in liver (9), and of acyl-coenzyme A oxidase 1 (ACOX1), a PPARα downstream target and a rate-limiting enzyme of peroxisomal fat oxidation, were both significantly increased in the liver of the $Rb^{+/-}$ mice (Fig. 8). Strikingly, the mRNA levels of the lipogenic transcription factor sterol regulatory element-binding protein-1c (SREBP-1c) and its target gene fatty acid synthase (FAS) were also increased in the liver of the

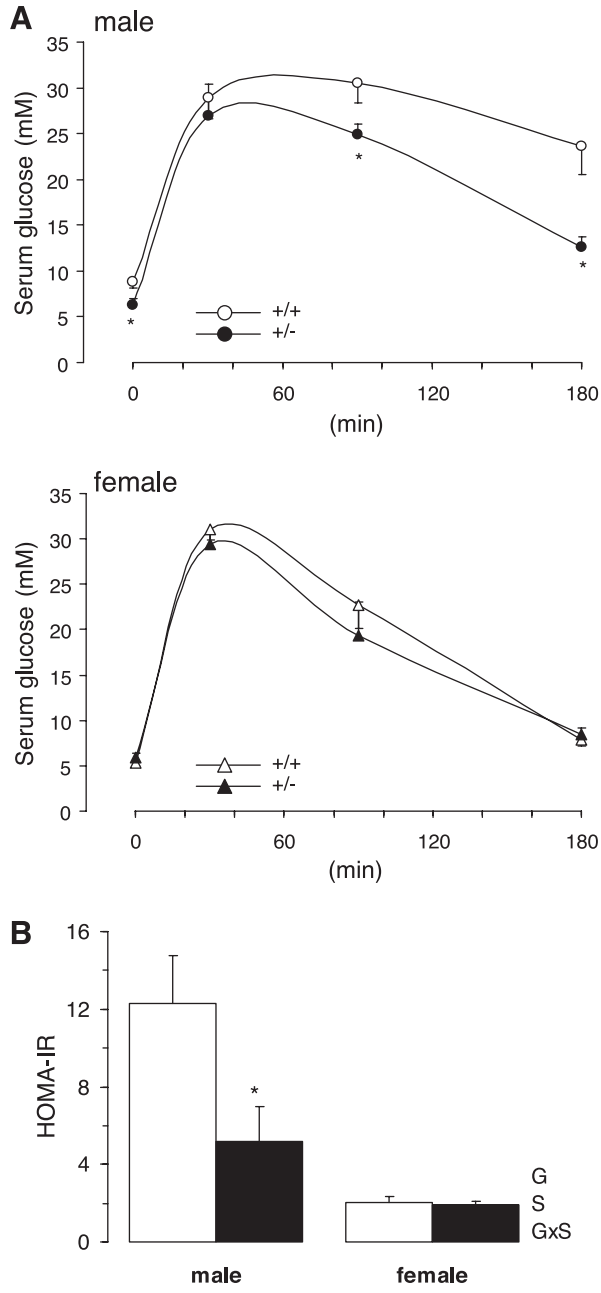

Fig. 3. Rb haploinsufficiency improves glucose tolerance and reduces insulin resistance after high fat-diet feeding in male mice. *A*: blood glucose profile following a glucose load in wild-type and $Rb^{+/-}$ mice after 14 wk on HFD60. *B*: homeostatic model assessement for insulin resistance (HOMA-IR) score in wild-type (open bars) and $Rb^{+/-}$ (filled bars) mice after 14 wk on HFD60. Data are the mean ± SE of 6 animals/group. G × S, significant effect of the interaction between genotype and sex in 2-way ANOVA ($P < 0.05$). *Different from sex-matched wild-type group ($P < 0.05$; Student's *t*-test).

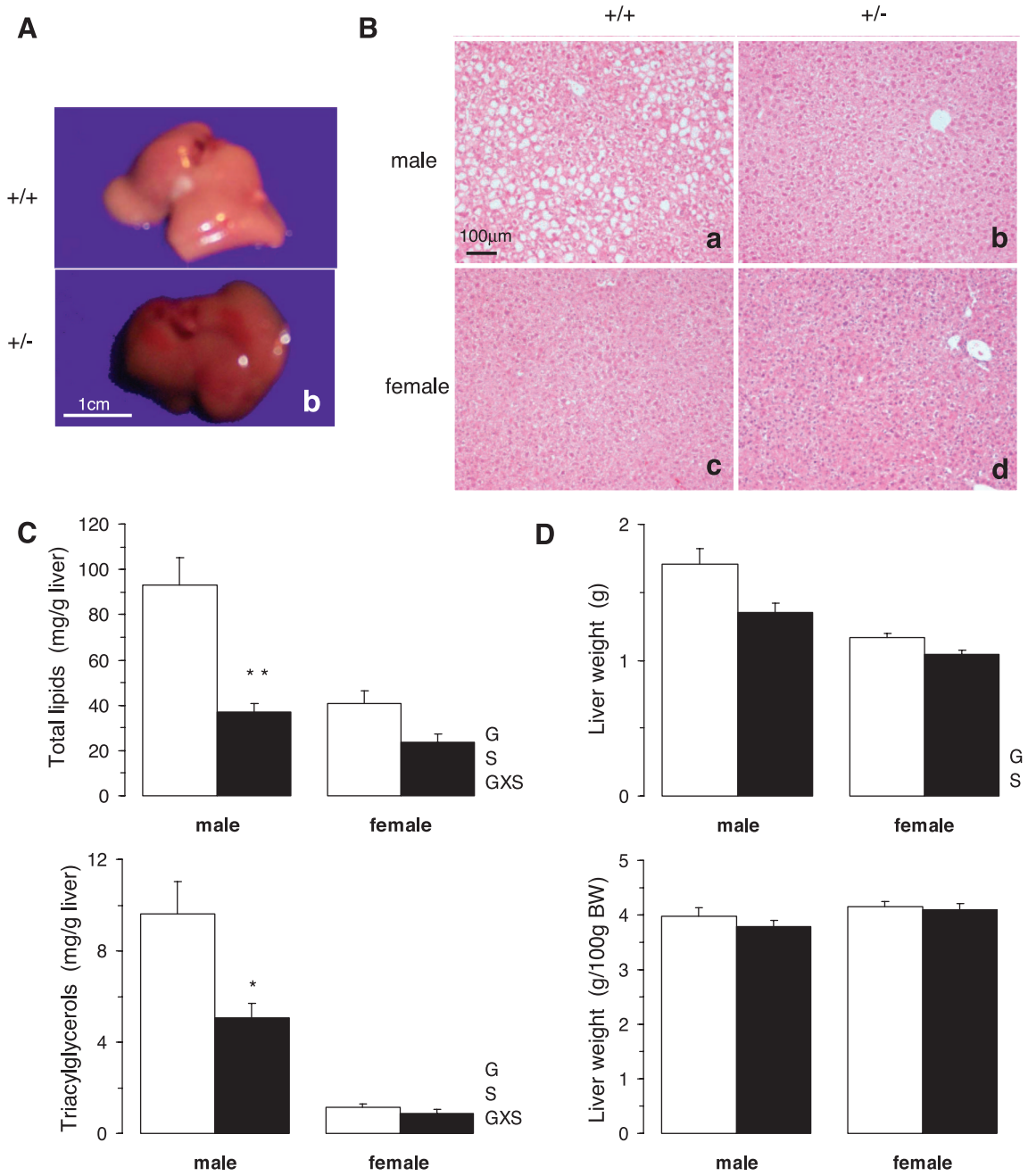

Fig. 4. Rb haploinsufficiency reduces hepatosteatosis after high-fat diet feeding in male mice. *A*: macroscopic appearance of liver in wild-type and $Rb^{+/-}$ male mice after 18 wk on HFD60. *B*: hematoxylin-eosin staining of liver sections in wild-type and $Rb^{+/-}$ mice after 18 wk on HFD60. *C*: total lipid and triacylglycerol content in liver of wild-type and $Rb^{+/-}$ mice after 18 wk on HFD60. *D*: absolute liver weights and liver weights/body weights in wild-type and $Rb^{+/-}$ mice after 18 wk on HFD60. Open bars, wild-type mice; filled bars, $Rb^{+/-}$ mice. Data are the mean ± SE of 6–10 animals/group. * and **Different from sex-matched wild-type group ($P < 0.05$ and $P < 0.01$, respectively; Student's *t*-test).

$Rb^{+/-}$ mice compared with wild-type littermates (Fig. 8). In skeletal muscle, $Rb^{+/-}$ mice had increased mRNA levels of PPARδ (relative expression to β-actin: 1.89 ± 0.17 vs. 1.19 ± 0.22, $P = 0.038$), suggestive of an increased capability for fatty acid oxidation (9), yet other fatty acid catabolism-related proteins examined, such as PGC-1α, muscle-type carnitine palmitoyl transferase I, ACOX1, uncoupling protein 3, acetyl-CoA-carboxylase 2, and fatty acid transporter CD36, were similarly expressed at the mRNA level regardless of the Rb genotype (data not shown).

Rb-Haploinsufficient Mice Have Increased PGC-1α Expression in WAT Compared With Wild-Type Mice of Equal Adiposity

Metabolic changes allowing resistance to diet-induced obesity could already have been present in the $Rb^{+/-}$ mice before changes in adiposity relative to wild-type littermates became evident. To test this, we performed gene expression analysis in WAT and BAT samples of $Rb^{+/-}$ and wild-type male mice of equal body adiposity (mice unchallenged with a high-fat diet or

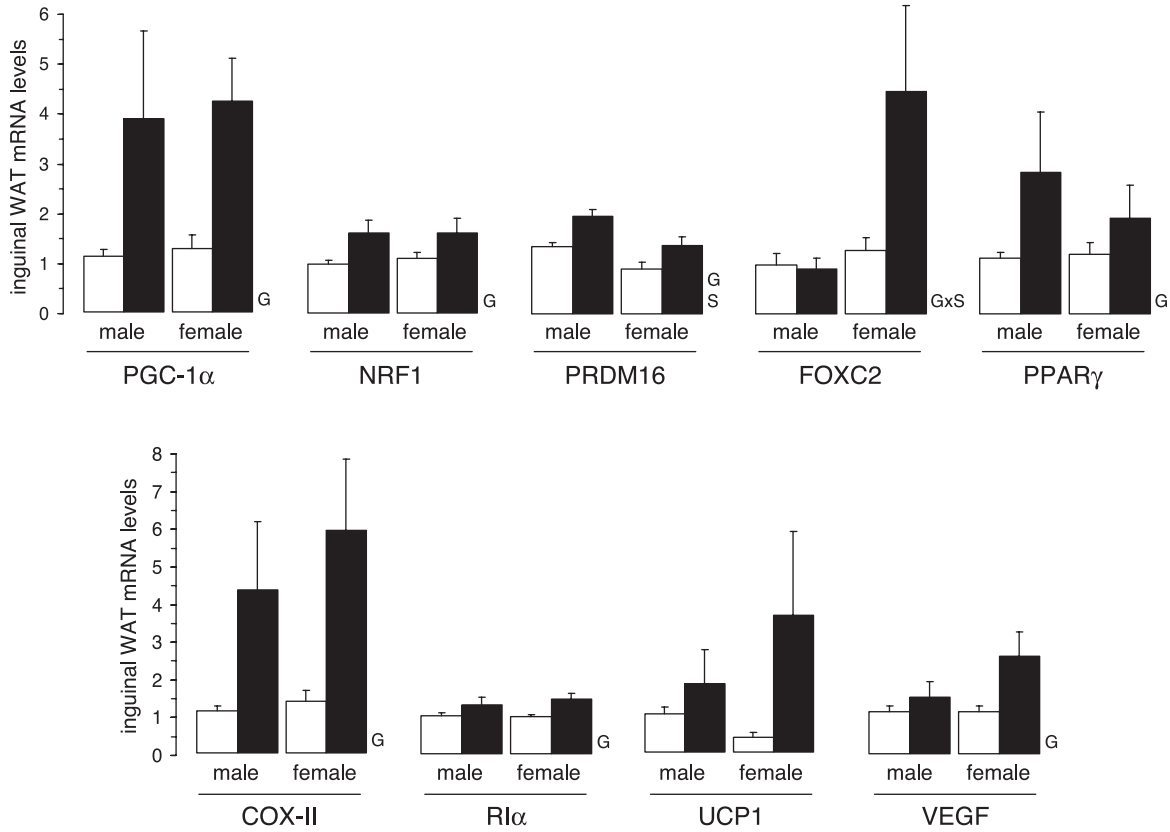

Fig. 5. Expression of selected genes in iWAT of $Rb^{+/-}$ and wild-type mice after 18 wk of HFD60. mRNA level data are given as expression relative to β-actin and are the mean ± SE of 6–10 animals/group. Open bars, wild-type mice; filled bars, $Rb^{+/-}$ mice. Two-way ANOVA. PGC-1α, peroxisome proliferator-activated receptor-γ (PPARγ) coactivator-1α; NRF1, nuclear respiratory factor 1; PRDM16, PR domain zinc finger protein 16; FOXC2, forkhead box C2; COX-II, cytochrome oxidase subunit II; RIα, cAMP-dependent protein kinase A regulatory subunit Iα; UCP1, uncoupling protein 1.

challenged with HFD45 during 12 wk). Expression levels of PGC-1α mRNA in inguinal WAT were already higher in the $Rb^{+/-}$ mice in the absence of a dietary challenge (relative expression to β-actin: 1.85 ± 0.24 vs. 1.10 ± 0.24, $P = 0.045$) and, more markedly, after HFD45 (relative expression to β-actin: 2.75 ± 0.55 vs. 0.93 ± 0.23, $P = 0.024$). No differences between $Rb^{+/-}$ and wild-type mice regarding BAT mRNA levels of thermogenesis-related genes (UCP1, PGC-1α, FOXC2) were detected under these conditions (data not shown). Levels of PPARγ mRNA in inguinal WAT were similar in both Rb genotype groups prior to high-fat diet feeding and higher in the $Rb^{+/-}$ mice after HFD45 (mRNA expression relative to β-actin: 2.05 ± 0.31 in $Rb^{+/-}$ mice vs. 1.16 ± 0.17 in wild-type mice, $P = 0.019$).

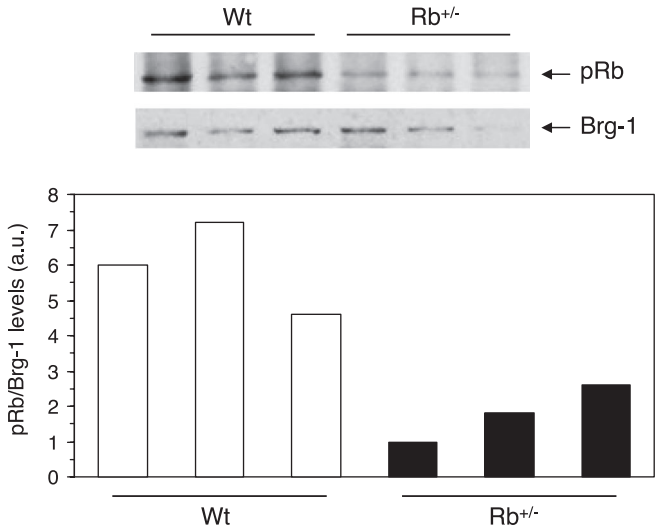

Fig. 6. Retinoblastoma protein (pRb) protein levels in iWAT from $Rb^{+/-}$ or wild-type mice. pRb protein levels were determined by immunoblotting, as described in MATERIALS AND METHODS in WAT samples from 4-mo-old $Rb^{+/-}$ or wild-type male mice fed a standard chow diet. Brg-1 served as a control for total homogenate protein loaded and blotted. The bar diagram corresponds to the densitometric scan of the *top blot*.

DISCUSSION

Results in this work provide first evidence that germ line Rb haploinsufficiency confers protection against the development of diet-induced obesity and obesity-associated metabolic disturbances (hepatosteatosis, systemic insulin resistance) after long-term high-fat diet feeding. Collectively, our data suggest that reduced dietary obesity in $Rb^{+/-}$ mice is attributable to increased energy expenditure and reduced feed efficiency coupled with increased BAT activity and energy metabolism in WAT. Recently, adipose tissue-specific homozygous ablation of the Rb gene in adult mice, using the loxP-$CreER^{T2}$ technology with expression of a tamoxifen-inducible Cre recombinase driven by the adipocyte-specific aP2 promoter, was shown to protect against high-fat diet-induced diabesity because of increased energy expenditure linked to mitochondrial activation in BAT and WAT (6). The current investigation adds insight into the physiological relevance of the pRb in the regulation of

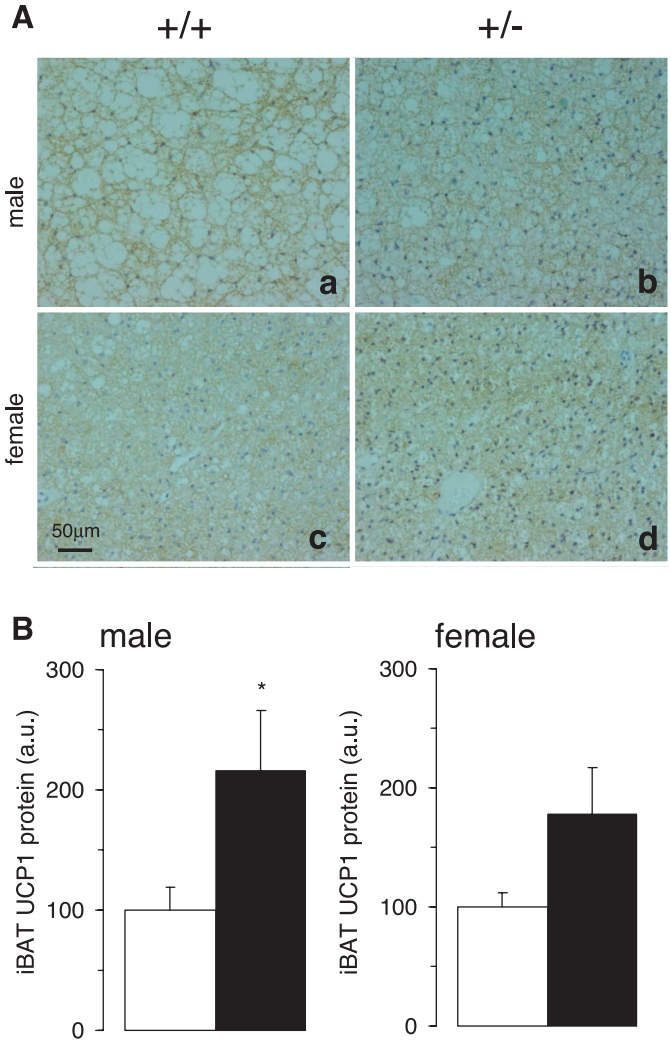

Fig. 7. *A*: hematoxylin-eosin staining of iBAT sections of wild-type and $Rb^{+/-}$ mice after 18 wk on a HFD60 also showing immunohistochemical detection of UCP1 (brown). *B*: UCP1 protein levels in iBAT of $Rb^{+/-}$ mice (filled bars) compared with sex-matched wild-type littermates (open bars) after 18 wk on HFD60. UCP1 was determined by immunoblotting. Data are the mean ± SE of 6–9 animals/group and are expressed relative to the mean value of the sex-matched wild-type group, which was set as 100%. *Different from sex-matched wild-type group ($P < 0.05$; Student's *t*-test).

whole body energy metabolism by revealing similar effects in a more physiological model of generalized partial deficiency throughout development. In addition, our work is the first to suggest that partial pRb deficiency may also be associated with increased fatty acid oxidation in nonadipose tissues (liver and skeletal muscle) in the context of a challenge with a high-fat diet.

Differences in WAT gene expression between $Rb^{+/-}$ and wild-type mice after HFD60 are in keeping with observed end points (reduced obesity and increased body temperature in the $Rb^{+/-}$ mice) and in line with an inhibitory action of pRb on the expression of brown adipocyte marker genes (6, 12, 33). Thus, in parallel with a reduced content in pRb protein, WAT depots of $Rb^{+/-}$ mice displayed an increased expression at the mRNA level of several genes related to mitochondrial biogenesis/function and uncoupling activity (PGC-1α, NRF1, COX-II, UCP1), cAMP sensitivity (FOXC2, RIα), and brown adipocyte determination (PRDM16). In particular, PGC-1α gene expression was markedly increased in WAT depots of $Rb^{+/-}$ mice both before and after high-fat diet feeding, which is in keeping with a report showing that pRb negatively regulated the PGC-1α gene promoter in differentiated 3T3-L1 white adipocytes (33). WAT depots of the $Rb^{+/-}$ mice also exhibited signs of increased vascularization (including increased VEGF mRNA levels), a feature that can contribute to support increased metabolism and to dissipate the heat produced thereof. Signs of a more active BAT in the $Rb^{+/-}$ mice after HFD60 were also evident, in keeping with their reduced development of dietary obesity compared with wild-type littermates, namely reduced lipid content and increased expression of UCP1 protein and RIα mRNA. In addition, higher mRNA expression levels of PPARα and ACOX1 in liver and of PPARδ in skeletal muscle are suggestive of a relatively increased capability for fatty acid oxidation in these tissues in the $Rb^{+/-}$ mice under a high-fat diet.

Rb haploinsufficiency resulted in the amelioration of high-fat diet-induced hepatosteatosis and insulin resistance in the male mice, in which these disturbances were much more marked than in the female mice. Thus, even if our experimental design was not intended to analyze sex-dependent responses to a high-fat diet, our results strongly suggest that female C57BL/6J mice are less prone than males to developing dietary obesity-linked disturbances, in keeping with findings in rats (24) and with observations in humans (28). Improved systemic insulin sensitivity after HFD60 in $Rb^{+/-}$ male mice relative to wild-type littermates was unrelated to differences in the circulating levels of the insulin-sensitizing hormone adiponectin or muscle triacylglycerol content and may be secondary to their reduced body fat, particularly liver fat, and circulating NEFA levels (36). The possibility that the pRb status impacts on insulin sensitivity through more direct mechanisms cannot be discarded since $Rb^{+/-}$ mice fed regular chow already display signs of increased systemic insulin sensitivity (they maintained normoglycemia at reduced insulinemia) in the absence of differences in body adiposity relative to wild-type littermates. In this context, it is of note that increased activation of components of the insulin-signaling pathway has been reported

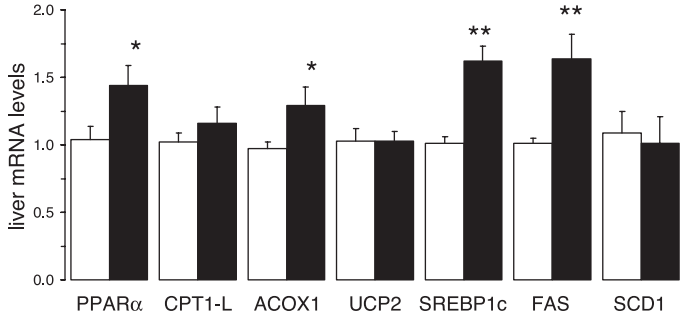

Fig. 8. Expression of fatty acid oxidation and lipogenesis-related genes in liver of $Rb^{+/-}$ and wild-type male mice after 18 wk of HFD60. mRNA levels data are given as expression relative to β-actin and are the mean ± SE of 6–9 animals/group. Open bars, wild-type mice; filled bars, $Rb^{+/-}$ mice. *Different from wild-type mice, $P < 0.05$, Student's *t*-test; **different from wild-type mice, $P < 0.001$, Student's *t*-test. CPT I-L, carnitine palmitoyl transferase I liver type; ACOX1, acyl-coenzyme A oxidase 1; SREBP-1c, sterol regulatory element-binding protein-1c; FAS, fatty acid synthase; SCD1, stearoyl-coenzyme A desaturase-1.

in Rb-deficient compared with wild-type mouse embryonic fibroblasts (13).

Simultaneously increased capabilities for adipogenesis/lipogenesis and fatty acid oxidation in critical tissues detected in this work suggest a possible explanation for the requirement of a prolonged dietary challenge to evidence a reduced adiposity in the $Rb^{+/-}$ mice, although signs of increased metabolism (increased rectal temperature, cold tolerance, and PGC-1α expression in WAT) were already present in these mutants when they were maintained on regular chow or fed a high-fat diet for shorter periods. In particular, we found the mRNA expression levels of PPARγ to be increased along with that of energy metabolism-related genes in WAT depots of the $Rb^{+/-}$ mice after different periods of high-fat diet feeding as well as evidence of increased capabilities for both lipogenesis (increased SREBP-1c and FAS expression) and fatty acid oxidation (increased PPARα and ACOX1 expression) in the liver of the $Rb^{+/-}$ mice compared with wild-type littermates. Increased expression of lipogenic genes in WAT and liver may reflect an enhanced sensitivity of these tissues to the lipogenic effects of insulin in the $Rb^{+/-}$ mice. The increased PPARγ expression in WAT of $Rb^{+/-}$ mice may also reflect derepression of PPARγ in the setting of partial Rb deficiency, since pRb can block the transcriptional activity of liganded PPARγ (8) and activation of PPARγ can result in increased PPARγ mRNA levels, as certain PPARγ target genes (e.g., C/EBPα) encode proteins known to transactivate the PPARγ gene promoter (32). A prolonged dietary challenge appears to create conditions under which the effects on energy expenditure finally prevail.

In summary, the findings in this work support a role for pRb modulating energy metabolism and the responses to long-term high-fat diet feeding by showing that pRb haploinsufficiency protects obesity-prone C57BL/6J mice against high-fat diet-induced obesity and its related complications of insulin resistance and hepatosteatosis.

ACKNOWLEDGMENTS

We thank Prof. Daniel Ricquier for the UCP1 antibodies, Teresa de Francisco for excellent assistance in the breeding of the animals, and Marc Corrales for help during animal growth followup.

GRANTS

This work was supported by the Spanish Government (Grant AGL2006-04887/ALI to A. Palou) and the Italian Government (FIRB Internazionalizzazione RBIN047PZY2005 to S. Cinti). The Laboratory of Molecular Biology, Nutrition, and Biotechnology, Universitat de les Illes Balears, is part of The European Nutrigenomics Organization (European Union Contract no. FOOD-CT-2004-506360). The Department of Biochemistry and Molecular Biology, University of Southern Denmark, and the Department of Biology, University of Copenhagen, are part of the Danish Obesity Research Centre supported by The Danish Council for Strategic Research (Grant no. 2101-06-0005) and is also supported by the Danish Natural Science Research Council and the Novo Nordisk Foundation. Centro de Investigación Biomédica en Red de Fisiopatología de la Obesidad y Nutrición is an initiative of the Instituto de Salud Carlos III. J. Mercader was the recipient of a predoctoral fellowship from the Spanish Government.

REFERENCES

1. **Cederberg A, Gronning LM, Ahren B, Tasken K, Carlsson P, Enerback S.** FOXC2 is a winged helix gene that counteracts obesity, hypertriglyceridemia, and diet-induced insulin resistance. *Cell* 106: 563–573, 2001.
2. **Clarke AR, Maandag ER, van Roon M, van der Lugt NM, van der Valk M, Hooper ML, Berns A, te Riele H.** Requirement for a functional Rb-1 gene in murine development. *Nature* 359: 328–330, 1992.
3. **Classon M, Kennedy BK, Mulloy R, Harlow E.** Opposing roles of pRB and p107 in adipocyte differentiation. *Proc Natl Acad Sci USA* 97: 10826–10831, 2000.
4. **Cummings DE, Brandon EP, Planas JV, Motamed K, Idzerda RL, McKnight GS.** Genetically lean mice result from targeted disruption of the RII beta subunit of protein kinase A. *Nature* 382: 622–626, 1996.
5. **Chen PL, Riley DJ, Chen Y, Lee WH.** Retinoblastoma protein positively regulates terminal adipocyte differentiation through direct interaction with C/EBPs. *Genes Dev* 10: 2794–2804, 1996.
6. **Dali-Youcef N, Mataki C, Coste A, Messaddeq N, Giroud S, Blanc S, Koehl C, Champy MF, Chambon P, Fajas L, Metzger D, Schoonjans K, Auwerx J.** Adipose tissue-specific inactivation of the retinoblastoma protein protects against diabesity because of increased energy expenditure. *Proc Natl Acad Sci USA* 104: 10703–10708, 2007.
7. **Delston RB, Harbour JW.** Rb at the interface between cell cycle and apoptotic decisions. *Curr Mol Med* 6: 713–718, 2006.
8. **Fajas L, Egler V, Reiter R, Hansen J, Kristiansen K, Debril MB, Miard S, Auwerx J.** The retinoblastoma-histone deacetylase 3 complex inhibits PPARgamma and adipocyte differentiation. *Dev Cell* 3: 903–910, 2002.
9. **Feige JN, Gelman L, Michalik L, Desvergne B, Wahli W.** From molecular action to physiological outputs: peroxisome proliferator-activated receptors are nuclear receptors at the crossroads of key cellular functions. *Prog Lipid Res* 45: 120–159, 2006.
10. **Felipe F, Bonet ML, Ribot J, Palou A.** Modulation of resistin expression by retinoic acid and vitamin A status. *Diabetes* 53: 882–889, 2004.
11. **Handschin C, Spiegelman BM.** Peroxisome proliferator-activated receptor gamma coactivator 1 coactivators, energy homeostasis, and metabolism. *Endocr Rev* 27: 728–735, 2006.
12. **Hansen JB, Jørgensen C, Petersen RK, Hallenborg P, De Matteis R, Bøye HA, Petrovic N, Enerbäck S, Nedergaard J, Cinti S, te Riele H, Kristiansen K.** Retinoblastoma protein functions as a molecular switch determining white versus brown adipocyte differentiation. *Proc Natl Acad Sci USA* 101: 4112–4117, 2004.
13. **Hansen JB, Petersen RK, Jørgensen C, Kristiansen K.** Deregulated MAPK activity prevents adipocyte differentiation of fibroblasts lacking the retinoblastoma protein. *J Biol Chem* 277: 26335–26339, 2002.
14. **Hansen JB, Petersen RK, Larsen BM, Bartkova J, Alsner J, Kristiansen K.** Activation of peroxisome proliferator-activated receptor gamma bypasses the function of the retinoblastoma protein in adipocyte differentiation. *J Biol Chem* 274: 2386–2393, 1999.
15. **Hsu SM, Raine L, Fanger H.** Use of avidin-biotin-peroxidase complex (ABC) in immunoperoxidase techniques: a comparison between ABC and unlabeled antibody (PAP) procedures. *J Histochem Cytochem* 29: 577–580, 1981.
16. **Jacks T, Fazeli A, Schmitt EM, Bronson RT, Goodell MA, Weinberg RA.** Effects of an Rb mutation in the mouse. *Nature* 359: 295–300, 1992.
17. **Lee S, Muniyappa R, Yan X, Chen H, Yue LQ, Hong EG, Kim JK, Quon MJ.** Comparison between surrogate indexes of insulin sensitivity and resistance and hyperinsulinemic euglycemic clamp estimates in mice. *Am J Physiol Endocrinol Metab* 294: E261–E270, 2008.
18. **Livak KJ, Schmittgen TD.** Analysis of relative gene expression data using real-time quantitative PCR and the 2[−Delta Delta C(T)] Method. *Methods* 25: 402–408, 2001.
19. **Lowell BB, Spiegelman BM.** Towards a molecular understanding of adaptive thermogenesis. *Nature* 404: 652–660, 2000.
20. **Matthews DR, Hosker JP, Rudenski AS, Naylor BA, Treacher DF, Turner RC.** Homeostasis model assessment: insulin resistance and beta-cell function from fasting plasma glucose and insulin concentrations in man. *Diabetologia* 28: 412–419, 1985.
21. **Mercader J, Madsen L, Felipe F, Palou A, Kristiansen K, Bonet ML.** All-trans retinoic acid increases oxidative metabolism in mature adipocytes. *Cell Physiol Biochem* 20: 1061–1072, 2007.
22. **Mercader J, Ribot J, Murano I, Felipe F, Cinti S, Bonet ML, Palou A.** Remodeling of white adipose tissue after retinoic acid administration in mice. *Endocrinology* 147: 5325–5332, 2006.
23. **Nguyen DX, McCance DJ.** Role of the retinoblastoma tumor suppressor protein in cellular differentiation. *J Cell Biochem* 94: 870–879, 2005.
24. **Priego T, Sanchez J, Pico C, Palou A.** Sex-differential expression of metabolism-related genes in response to a high-fat diet. *Obesity (Silver Spring)* 16: 819–826, 2008.
25. **Puigserver P, Nadal-Ginard B, Palou A.** Expression and interaction of C/EBPalpha adipogenic transcription factor and retinoblastoma protein in adipocytes during differentiation (Abstract). *Int J Obes Relat Metab Disord* 18: 113, 1994.

26. **Puigserver P, Ribot J, Serra F, Gianotti M, Bonet ML, Nadal-Ginard B, Palou A.** Involvement of the retinoblastoma protein in brown and white adipocyte cell differentiation: functional and physical association with the adipogenic transcription factor C/EBPalpha. *Eur J Cell Biol* 77: 117–123, 1998.
27. **Puigserver P, Spiegelman BM.** Peroxisome proliferator-activated receptor-gamma coactivator 1 alpha (PGC-1 alpha): transcriptional coactivator and metabolic regulator. *Endocr Rev* 24: 78–90, 2003.
28. **Regitz-Zagrosek V, Lehmkuhl E, Weickert MO.** Gender differences in the metabolic syndrome and their role for cardiovascular disease. *Clin Res Cardiol* 95: 136–147, 2006.
29. **Ribot J, Oliver P, Serra F, Palou A.** Retinoic acid modulates the retinoblastoma protein during adipocyte terminal differentiation. *Biochim Biophys Acta* 1740: 249–257, 2005.
30. **Rodriguez-Sureda V, Peinado-Onsurbe J.** A procedure for measuring triacylglyceride and cholesterol content using a small amount of tissue. *Anal Biochem* 343: 277–282, 2005.
31. **Rosen ED.** The transcriptional basis of adipocyte development. *Prostaglandins Leukot Essent Fatty Acids* 73: 31–34, 2005.
32. **Rosen ED, Walkey CJ, Puigserver P, Spiegelman BM.** Transcriptional regulation of adipogenesis. *Genes Dev* 14: 1293–1307, 2000.
33. **Scime A, Grenier G, Huh MS, Gillespie MA, Bevilacqua L, Harper ME, Rudnicki MA.** Rb and p107 regulate preadipocyte differentiation into white versus brown fat through repression of PGC-1alpha. *Cell Metab* 2: 283–295, 2005.
34. **Seale P, Kajimura S, Yang W, Chin S, Rohas LM, Uldry M, Tavernier G, Langin D, Spiegelman BM.** Transcriptional control of brown fat determination by PRDM16. *Cell Metab* 6: 38–54, 2007.
35. **Shao D, Lazar MA.** Peroxisome proliferator activated receptor gamma, CCAAT/enhancer-binding protein alpha, and cell cycle status regulate the commitment to adipocyte differentiation. *J Biol Chem* 272: 21473–21478, 1997.
36. **Wilding JP.** The importance of free fatty acids in the development of Type 2 diabetes. *Diabet Med* 24: 934–945, 2007.